Adsorption of Block Copolymers in Nanoporous Alumina

SOTIRIA KARAGIOVANAKI,[1] ALEXANDROS KOUTSIOUBAS,[1] NIKOLAOS SPILIOPOULOS,[1] DIMITRIS L. ANASTASSOPOULOS,[1] ALEXANDROS A. VRADIS,[1] CHRIS TOPRAKCIOGLU,[1] ANGELIKI ELINA SIOKOU[2]

[1]Department of Physics, University of Patras, Patras 26500, Greece

[2]Foundation for Research and Technology, Institute of Chemical Engineering and High Temperature Chemical Processes (FORTH/ICE-HT), Hellas, Stadiou Str., Platani, P.O. Box 1414, GR-26504 Patras, Greece

Received 20 October 2009; revised 23 December 2009; accepted 29 December 2009
DOI: 10.1002/polb.21972
Published online in Wiley InterScience (www.interscience.wiley.com).

ABSTRACT: We have studied the adsorption of end-attaching block copolymer chains inside the cylindrical pores of nanoporous alumina. Highly asymmetric PS-PEO block copolymers, with a small PEO anchoring block and a long PS dangling block, were allowed to adsorb onto porous alumina substrates with an average pore diameter of ~200 nm from toluene solution. The adsorption process was monitored using FTIR spectroscopy, whereas depth profile analysis was performed by means of XPS and Ar^+ ion sputtering. It is found that the PS-PEO adsorption kinetics in porous alumina are ~4 orders of magnitude slower than the corresponding case of a flat alumina substrate. It appears that chains adsorbed near the pore entrance early on tend to form a barrier for chains entering the pore at later times, thereby slowing down the adsorption process significantly. This effect is much more pronounced for large chains whose dimensions are comparable with the pore diameter. The equilibrium adsorbance value is also affected by chain size due to the additional entropic penalty associated with chain confinement, the adsorbance falling substantially when the chain dimensions become comparable with the pore diameter. © 2010 Wiley Periodicals, Inc. J Polym Sci Part B: Polym Phys 48: 1676–1682, 2010

KEYWORDS: adsorption; block copolymers; nanolayers; polymer brush; porous alumina

INTRODUCTION Flexible polymer chains end-attached to a surface in good solvent tend to extend away from the surface at sufficiently high grafting density, as a result of excluded volume interactions, to form a layer of stretched chains known as a "polymer brush." Such systems have been the subject of extensive theoretical and experimental studies[1] due to their various applications in colloidal stabilization, adhesion, wetting, and lubrication as well as tailoring surface properties and the development of responsive nanomaterials.[2] In recent years, the properties of polymer brushes formed on convex or concave interfaces have been studied using theory or simulation.[3–15] Scaling theory,[3–7] Monte Carlo,[7–12] and molecular dynamics simulations[13,14] have been used for this purpose. These investigations include various structures with a confined geometry such as cylindrical pores,[5,6,11] tubes,[3,7,10,13] channels,[12] slits,[9,14] spherical cavities,[8] convex surfaces,[4] and other complex structures.[15] Although numerous theoretical and simulation studies have been reported in this area,[3–15] relatively few experimental investigations appear to have been carried out.[16] The aim of this article is to attempt to bridge this gap.

A versatile template for the experimental study of adsorption in a cylindrical geometry is porous anodic alumina membranes. Porous anodic alumina (PAA) is formed by the electrochemical oxidation of aluminum under well-defined conditions of electrolyte, temperature, and voltage. Anodization parameters such as anodization voltage, current, anodization time, electrolyte bath temperature, and composition are all suitably adjusted during the fabrication of the template to obtain the desired distribution, size, and length of the pores. With the proper choice of these conditions, the generated film has a unique morphology of a honeycomb array of tubes, which are perpendicular to the surface of the film. In recent years, PAA has attracted much interest in both scientific and commercial fields as an indispensable part of nanotechnology for the fabrication of several kinds of nanodevices. PAA has found applications in filters, collimators, as a template for nanopatterning and nanowire growth, and as a photonic bandgap material.[17–21] Applications in the fields of electronics or optoelectronics, dense magnetic storage, energy storage, catalysis, nanoelectrodes, field emission devices, thermoelectric devices, photovoltaic devices, photonics, and biosensors, and the study of low-dimensional quantum effects have also been reported.[22–25] Several researchers have also used PAA as a mask for etching or deposition processes.

In this article, we report results for the adsorption of polystyrene-polyethyleneoxide (PS-PEO) block copolymers in the confined geometry of cylindrical pores that leads to the formation of polymer brushes on the pore walls of nanoporous alumina. Considerable experimental work has been reported in recent years on the adsorption of PS-PEO block

Correspondence to: C. Toprakcioglu (E-mail: ctop@physics.upatras.gr)

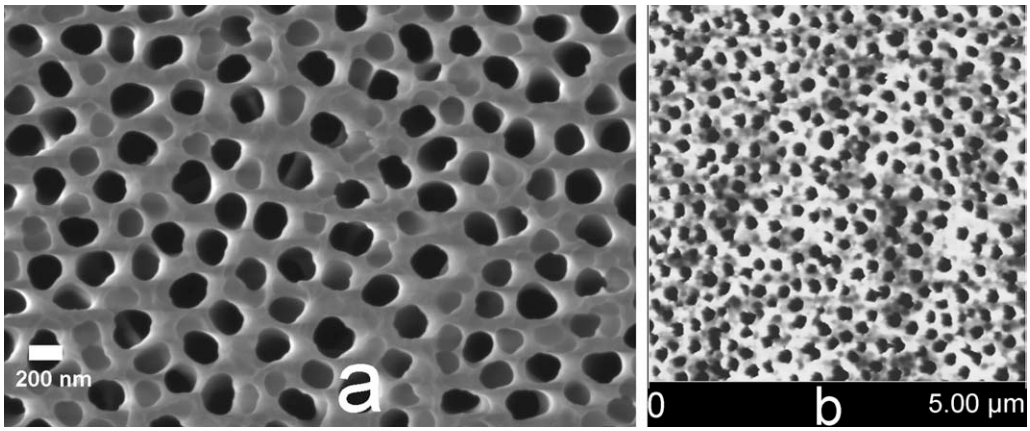

FIGURE 1 (a) SEM and (b) AFM images of the surface of porous alumina disks.

copolymers on flat oxide surfaces such as SiO_2 and Al_2O_3 and their behavior is now well-understood.[26–29] Therefore, these systems are suitable candidates for investigations aiming to explore the effects of a confined geometry on adsorption. It is known that such PS-PEO copolymers adsorb onto alumina via their PEO anchoring blocks from toluene, which is a good solvent for PS.[26–29]

EXPERIMENTAL

It is well-established that under suitable anodization conditions thin films of aluminum can be oxidized electrochemically to produce nanoporous Al_2O_3 with nearly monodisperse arrays of parallel pores having diameters typically in the range ~10–200 nm.[18,22] Porous alumina disks with a mean pore size of ~200 nm, a porosity of ~30–40%, and a thickness of 60 μm were obtained from Whatman and used as substrates for adsorption. The surface of these porous alumina membranes was examined by scanning electron microscopy (SEM) and atomic force microscopy (AFM) (see Fig. 1). Both techniques reveal the presence of a moderately regular pattern of pores with an average diameter of ~200 nm. Although no two alumina disks are identical, we found that the average pore size showed only a small variation (ca. ±5–10%) between disks, whereas the porosity was 35–40%. The cross-sectional SEM images (not shown) further reveal a pattern of parallel cylindrical pores with virtually no branching in any of the examined samples.

Highly asymmetric PS-PEO block copolymers with long PS chains and short PEO blocks were purchased from Polymer Laboratories (see Table 1). Toluene was used as a solvent to prepare solutions of the block copolymers. Adsorption was allowed to take place by first immersing the alumina disks in toluene and then adding solution to the pure solvent so as to obtain the desired bulk concentration, which was in the range 0.05–0.5 mg/mL. Adsorption times varied from 30 min to 2 months. Adsorption was monitored by FTIR spectroscopy. To record a spectrum, the alumina disks were removed from the solution, rinsed with pure toluene, allowed to dry under ambient conditions, and then measured using a Bruker Vector 22 FTIR spectrometer. Adsorbance, Γ, values were calculated from the measured FTIR absorbance of the C—H stretching peak at 2924 ± 2 cm^{-1} after calibration with a standard PS sample. The pore surface area was estimated from the mean pore diameter and interpore separation of the porous alumina membranes.

X-ray photoelectron spectroscopy (XPS) experiments were carried out in an ultrahigh vacuum system (UHV), which consists of a fast entry specimen assembly, a sample preparation, and an analysis chamber.[30] The base pressure in both chambers was 1×10^{-9} mbar. An unmonochromatized AlKα line at 1486.6 eV and an analyzer pass energy of 97 eV, giving a full width at half maximum (FWHM) of 1.7 eV for the Au $4f_{7/2}$ peak, were used in all XPS measurements. The XPS core level spectra were analyzed using a fitting routine, which can decompose each spectrum into individual mixed Gaussian-Lorentzian peaks after a Shirley background subtraction. Regarding the measurement errors, for the XPS core level peaks, we estimate that for a good signal to noise ratio, errors in peak positions are about ±0.05 eV. The binding energy (BE) scale was calibrated by assigning the main C1s peak at 284.6 eV.

Depth profile measurements were performed by XPS and revealed the in-depth distribution of chemical species of the sample. The surface was sputtered by Ar^+ ions (HV = 5 kV, $P_{Ar} \sim 4 \times 10^{-6}$ mbar) for certain time intervals, tsp, in particular tsp = 1 min for the film's top part and tsp = 3–5 min for film's deeper regions. A set of XPS peaks Al2p, C1s,

TABLE 1 Molecular Characteristics of PS-PEO Block Copolymers

Polymer	Mol. Wt. (kg/mol)	% PEO	M_w/M_n	R_F (nm) in Toluene
PS-PEO 80 K	80	5.0	1.07	24
PS-PEO 147 K	147	1.3	1.09	34
PS-PEO 183 K	183	4.2	1.07	38
PS-PEO 322 K	322	2.4	1.19	53
PS-PEO 497 K	497	1.2	1.18	69

and O1s was recorded after each sputtering step. For the calibration of the sputtered depth, an ultra thin ($d = 17$ nm) Al_2O_3 film prepared by Thermal Evaporation on Al wafer was used. The film was sputtered until the Al2p signal from the metallic Al substrate was maximized and the O1s and Al2p intensities from the oxidized over-layer were minimized. From this procedure, the sputtering rate of the Al_2O_3 was found to be $\sim 0.7 \pm 0.1$ nm/min. This value was used for the approximate estimation of the sputtered depth in this case. It is expected that the present sputtering conditions are destructive for the polymer, but this does not affect the quantitative analysis of the depth profile measurements.

RESULTS AND DISCUSSION

When block copolymers are allowed to adsorb from a selective solvent onto a flat solid substrate their surface concentration rises as adsorption proceeds, resulting in increased repulsion between neighboring nonadsorbing blocks in good solvent. This process continues and the chains become increasingly stretched until the repulsion experienced by the nonadsorbing blocks is exactly matched by the adsorption energy. Thus, at equilibrium the grafting density of the polymer brush is determined by this balance between the osmotic repulsion of the dangling blocks and the sticking energy of the adsorbing block.

However, the situation is more complicated in confined geometries, because chains have to pay an additional entropic penalty. For example, the free energy of confinement in a cylindrical pore for a nonadsorbing chain in good solvent is

$$F \sim kT(R_F/D)^{5/3} \quad (1)$$

where R_F is the Flory radius and D is the pore diameter. Clearly, when $D \ll R_F$, the confinement penalty can be large.

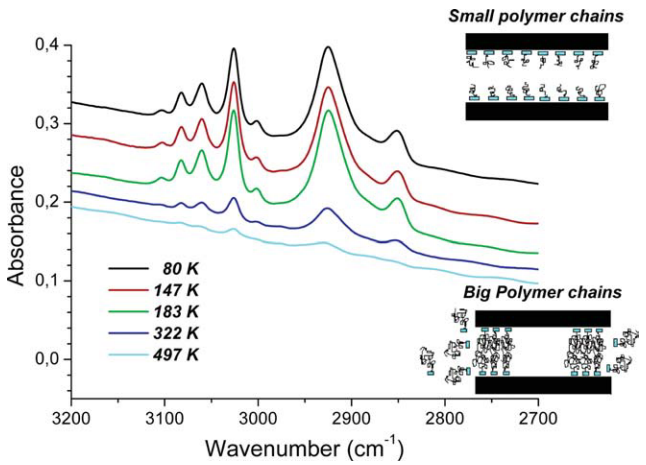

FIGURE 2 FTIR spectra of PS-PEO block copolymers end-adsorbed onto porous alumina of 200 nm mean pore size from an incubating solution at a concentration of 0.5 mg/mL in toluene. Adsorption time: 24 h. The adsorbed amount drops sharply for the high molecular weight polymers. The spectra have been offset for reasons of clarity.

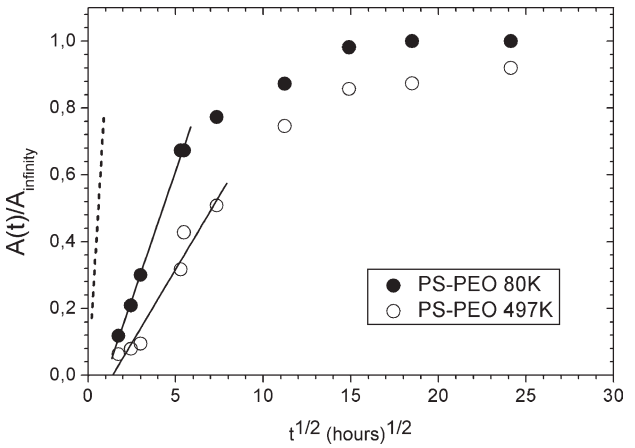

FIGURE 3 Normalized absorbance $A(t)/A_{infinity}$ of FTIR spectra as a function of the square root of adsorption time. Each set of symbols refers to the adsorption kinetics of a different copolymer onto porous alumina (200 nm mean pore size) as noted in the inset. Only two molecular weights are shown for reasons of clarity. The straight lines indicate the Fickian regime observed at small times for each copolymer. The bulk concentration is 0.1 mg/mL. The broken line indicates the corresponding behavior of the 497 K block copolymer on a flat alumina surface.

One may thus expect both the adsorbed amount at equilibrium as well as the kinetics of adsorption and brush formation to be strongly affected by the constraints imposed upon the adsorbing chains by confinement.

To study these effects, we have investigated the adsorption of highly asymmetric PS-PEO block copolymers whose macromolecular characteristics are summarized in Table 1. It is known from previous studies that when they adsorb on surfaces such as SiO_2 or Al_2O_3 from toluene, the sticking energy of the PEO anchoring blocks of these polymers is

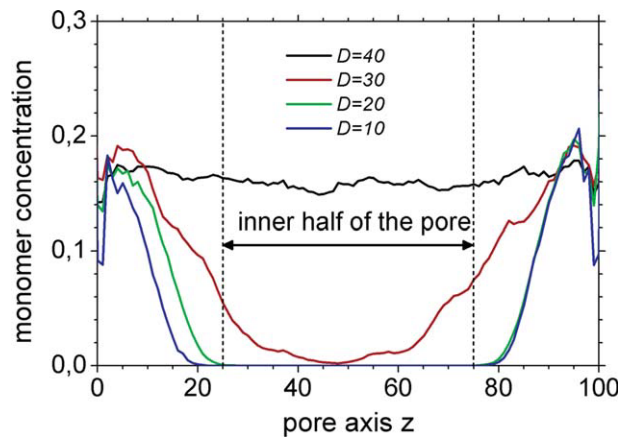

FIGURE 4 BFMC simulation result for monomer concentration along pore axis after 10^8 MC steps per monomer for chains consisting of 10 monomers ($N = 10$) and different pore diameters D. Note that a uniform concentration throughout the pore is achieved only for $D = 40$ (i.e., when the chain size is small compared with the pore diameter), (see ref. 34).

$\sim$7–8 kT.[26,27,29] As shown in Table 1, the Flory radii of the larger block copolymers are comparable with, though still smaller, the pore radii ($\sim$100 nm) of the confining alumina pores.

Adsorption Kinetics

Figure 2 shows the FTIR spectra obtained after 24 h incubation of the nanoporous alumina substrates in a toluene solution of the corresponding block copolymers at a concentration of 0.5 mg/mL in each case. Although the adsorbance values reached in 24 h are far from their saturation values, it is clear that the smaller copolymers, whose Flory radii are small in comparison with the pore radii, adsorb readily, but adsorption is much slower for the larger end-adsorbing macromolecules, whose characteristic dimensions are comparable with the pore diameter. It is evident that the block copolymers with the higher molecular weights show substantially reduced adsorption in comparison with their lower molecular weight counterparts over the same time period. This can be attributed to the considerably greater difficulty these larger macromolecules experience in their entry into a pore, especially after the very early stages of adsorption, when pores already contain some adsorbed polymers near the pore entrance.

If adsorption is allowed to proceed beyond 24 h, it is found that the adsorbance continues to rise until it eventually reaches a plateau at very long times that may extend over several days to weeks depending on the molecular weight of the block copolymers and the bulk concentration. As might be expected, at short times the adsorption kinetics exhibit a Fickian or diffusion controlled regime, with the adsorbance increasing with the square root of time[31]

$$\Gamma(t) = (2/\pi^{1/2})c_0(Dt)^{1/2} \qquad (2)$$

where Γ is the adsorbance, D is the diffusion coefficient, and c_0 is the bulk concentration. This behavior is shown in Figure 3. For a given value of c_0, one may obtain the corresponding diffusion coefficient, D, from the gradients of the linear parts of the curves at short times. Thus, it is possible to extract D-values of 1.3×10^{-10} cm^2 s^{-1} and 1.9×10^{-11} cm^2 s^{-1} for the 80 K and 497 K polymers, respectively. These values for the diffusion constant are roughly 4 orders of magnitude lower than the corresponding values obtained for adsorption of the same polymers on flat alumina substrates.[26] The dramatically reduced rates of diffusion in nanoporous alumina are clearly a consequence of geometric confinement.

To gain some further insight into this situation, we have carried out Bond Fluctuation Monte Carlo (BFMC) simulations based on the methodology of Carmesin and Kremer.[32,33] These simulations have been described in detail by Koutsioubas et al.[34] Briefly, after equilibration of two chain-containing reservoirs interconnected via a cylindrical pore, the pore entrances are "opened" and the chains are left free to enter the pore, whereas one of their two terminal monomers may adsorb irreversibly on the pore wall.

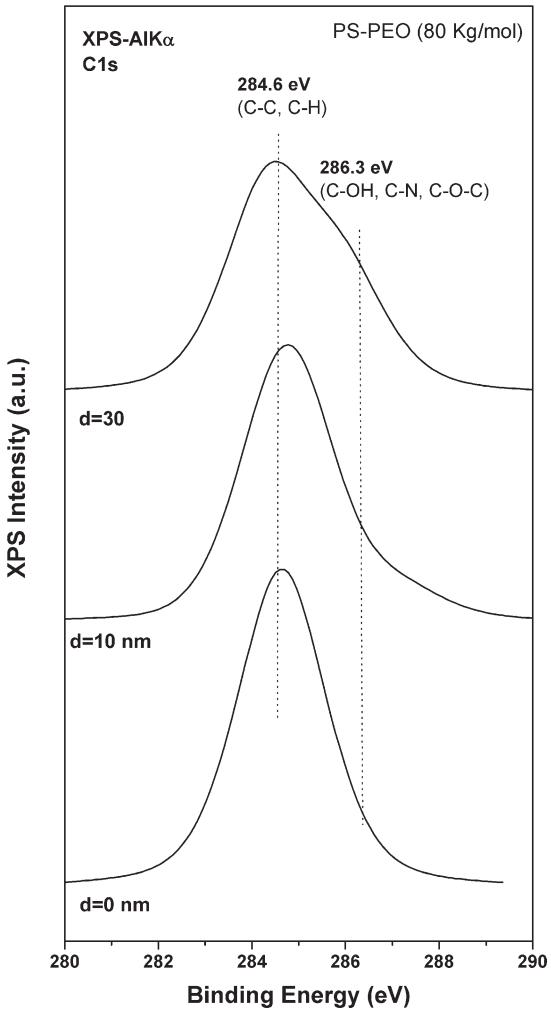

FIGURE 5 XPS C1s spectra recorded at three different moments during the Ar^+ sputtering procedure. The bottom spectrum corresponds to the surface of the sample, with the PS-PEO (80 kg/mol) copolymer, as received and is considered as d (depth) = 0 nm. It consists only of a single peak at 284.6 eV. During sputtering, a shoulder appears at the high binding energy side (middle spectrum, d = 10 nm) and becomes more prominent at about 30 nm in depth.

The results of the simulation are presented in Figure 4, which shows the monomer concentration along the pore axis after 10^8 Monte Carlo (MC) steps per monomer as a function of pore diameter, D, for chains consisting of 10 monomers each ($N = 10$). As the chains diffuse randomly into the pore, some chains become attached via one of their two ends to the pore wall. Because adsorption is assumed irreversible, once a chain has become attached, it remains so indefinitely. Thus, chains that have adsorbed near the pore entrance early on constitute an obstacle for chains arriving later.

Clearly, when the pore diameter becomes comparable with the chain size, adsorption is not uniform throughout, but is mainly concentrated near the pore entrances thus creating a barrier for incoming chains. The result is a "pore-plugging"

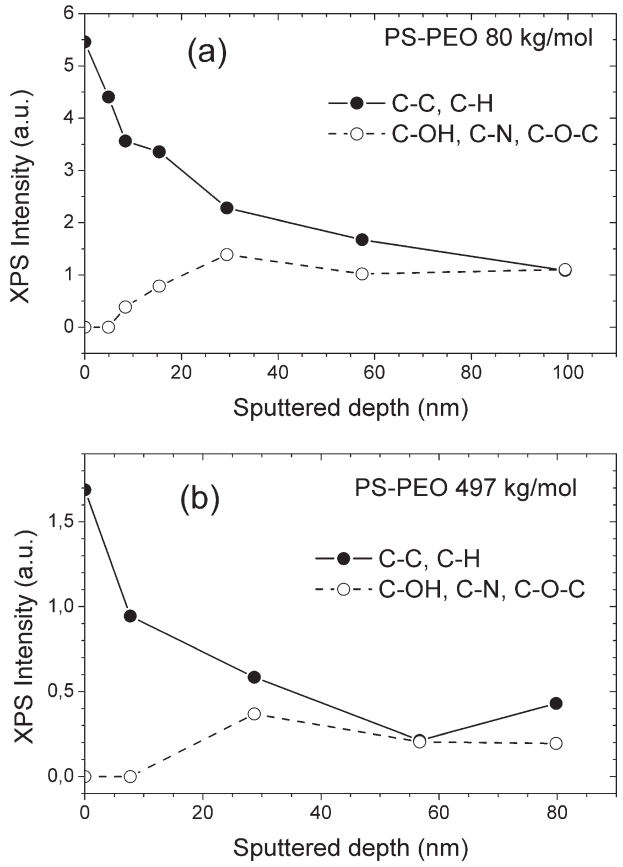

FIGURE 6 Depth profile of the C1s XPS peak intensities for (a) 80 kg/mol and (b) 497 kg/mol PS-PEO block copolymers after 24 h adsorption.

effect that dramatically slows down the kinetics of adsorption far from equilibrium. This is in qualitative agreement with the reduced adsorbance shown in Figure 3 for the larger polymers in the early stages of adsorption. Although the adsorption process of the PS-PEO block copolymers is not irreversible (the adsorption energy is ~7–8 kT[26,27,29]) and the entire length of the pore walls does eventually become populated by adsorbed chains at sufficiently long times, "pore-plugging" is still expected to play a significant role in slowing down the adsorption kinetics.

Depth profile analysis was carried out for the 80 K and 497 K PS-PEO block copolymers in an effort to probe the concentration of chains inside the cylindrical pores. In the case of the 80 K PS-PEO block copolymer, the C1s XPS peak appears initially at a binding energy (BE) of 284.6 eV. This energy is characteristic for C—C and C—H configurations and apart from the polymer chains it may also be attributed to carbon-containing contamination molecules on the outer surface of the samples. As shown in Figure 5 after the initial sputtering steps, a second C1s component appears at BE = 286.6 eV representing C—O—C, C—O—H, and/or C—N configurations. The behavior of the C1s peak during the sputtering procedure of the other sample with the 497 K PS-PEO block copolymer is similar. This component is almost certainly due to the PEO monomers of the PS-PEO block copolymer and is arguably a better identifier of the polymer chains that differentiates them from likely surface contaminants containing C—C and C—H. Although the intensity of the first component decreases in depth [Fig. 6(a)], the 2nd one increases and after the first 40–50 nm both intensities appear to reach a plateau. For the larger polymer (497 K) [Fig. 6(b)], it is possible that the concentration may still be falling, but more measurements are required at greater depth to establish this unambiguously. The observed features appear consistent with a picture where the anchoring blocks of the chains are attached to the pore walls, whereas at the pore entrance, one may expect dangling chains to be in abundance due to the presence of block copolymer chains adsorbed just outside the pores on the flat surface of the alumina membranes.

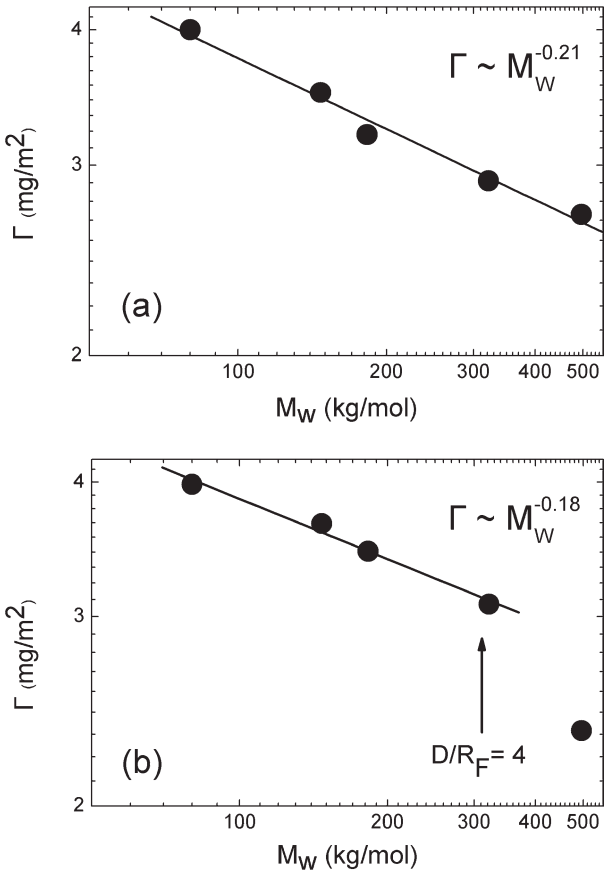

FIGURE 7 Plot of the final adsorbed amount versus PS-PEO copolymer molecular weight. (a) Adsorption on flat alumina measured by surface plasmon resonance techniques (see ref. 26). (b) Adsorption on porous alumina measured by FTIR spectroscopy (current work). The same PS-PEO block copolymers were used in both studies. The exponents of the power law, 0.21 ± 0.02 and 0.18 ± 0.02 for the flat and cylindrical geometries, respectively, are determined by a linear fit to each data set. Note the drop in adsorbance for the highest molecular weight polymer, whose dimensions are comparable with the pore radius. The arrow indicates the position where $D/R_F = 4$.

TABLE 2 Adsorption on Flat Alumina, Γ_{flat}, Measured by Surface Plasmon Resonance Experiments (ref. 26) and on Porous Alumina, Γ_{pore}, Measured by FTIR Spectroscopy (Current Work)

M_w (kg/mol)	Γ_{flat} (mg/m^2)	Γ_{pore} (mg/m^2)	σ^*_{flat}	σ^*_{pore}
80	4.0	4.0	8.9	8.9
147	3.5	3.7	8.7	9.2
183	3.2	3.5	8.3	9.1
322	2.9	3.1	8.3	8.8
497	2.7	2.3	8.4	7.1

Γ_{pore} values were calculated using specific surface area values estimated from the SEM images described in the Experimental section. The reduced coverage, σ^*, has been calculated using the expression $\sigma^* = \pi R_g^2/s^2$ (ref. 35), where $R_g = 0.0117\ M_w^{0.595}$ nm (ref. 36).

Equilibrium Adsorbance

In the case of PS-PEO block copolymer adsorption on flat substrates, the adsorbance values at saturation exhibit a molecular weight dependence.[26,28] For end-functionalized chains bearing a suitable anchoring group or for block copolymers with a short anchoring block, if the sticking energy is kept fixed but the molecular weight of the dangling block allowed to vary then simple scaling arguments suggest that $\Gamma \sim M^{-1/5}$ in agreement with what is observed experimentally[26,28] [see Fig. 7(a)]. Table 2 and Figure 7(b) show the dependence of D on molecular weight for the case of nanoporous alumina. The adsorbance is seen to fall with increasing molecular weight with an exponent close to the theoretically predicted value of 0.2 for the lower molecular weights, but the largest polymer deviates significantly from this pattern. These results suggest that although the PS-PEO block copolymer brushes require much longer times to form inside the cylindrical pores of alumina (as discussed earlier) in comparison with a flat alumina surface, their grafting densities at equilibrium are not strongly perturbed by confinement provided the chain dimensions are small relative to the pore diameter. It should be noted that the Flory radius of the largest polymer (497 K) is ~70 nm (see Table 1) and thus comparable with the pore radius (~100 nm). Furthermore, it is interesting to point out that the deviation occurs approximately at $D/R_F = 4$ [see Fig. 7(b)].

CONCLUSIONS

We have shown that the adsorption of terminally anchored chains that leads to the formation of a polymer brush in the confined geometry of a cylinder is much slower than the corresponding case of a flat substrate and depends strongly on the ratio of chain size to pore diameter with greatly reduced rates of adsorption for larger polymers. It appears that chains adsorbed near the pore entrances early on tend to form an effective barrier for chains entering the pores at later times, thereby slowing down the adsorption process significantly. The equilibrium adsorbance of such chains is also significantly affected by confinement, when the chain dimensions are comparable with the pore diameter, resulting in a reduced adsorbance and hence a lower grafting density. These effects may find potentially interesting applications such as in size exclusion processes, controlled release, and nanofluidics, and further work is under way to explore these aspects.

REFERENCES AND NOTES

1 Polymer Brushes: Synthesis, Characterization, Applications; Advincula, R. C.; Brittain, W. J.; Caster, K. C.; Rühe J., Eds.; Wiley-VCH: Weinheim, 2004.

2 Minko, S. Polym Rev 2006, 46, 397–420.

3 Manghi, M.; Aubouy, M.; Gay, C.; Ligoure, C. Eur Phys J E 2001, 5, 519–530.

4 Zhulina, E. B.; Birshtein, T. M.; Borisov, O. V. Eur Phys J E 2006, 20, 243–256.

5 Dimitrov, D.; Milchev, A.; Binder, K. Macromol Symp 2007, 252, 47–57.

6 Dimitrov, D.; Milchev, A.; Binder, K. J Chem Phys 2006, 125, 034905 1–034905 15.

7 Kremer, K.; Binder, K. J Chem Phys 1984, 81, 6381–6394.

8 Prochazka, K. J Phys Chem 1995, 99, 14108–14116.

9 Milchev, A.; Binder, K. J. Physique II 1996, 6, 21–32.

10 Avramova, K.; Milchev, A. J Chem Phys 2006, 124, 024909 1–024909 8.

11 Chen, S. B. J Chem Phys 2005, 123, 074702-1–074702-7.

12 Teraoka, I.; Wang, Y. Polymer 2004, 45, 3835–3843.

13 Dimitrov, D. I.; Milchev, A.; Binder, K. Heermann, D. W. Macromol Theory Simul 2006, 15, 573–583.

14 Dimitrov, D. I.; Milchev, A.; Binder, K.; Klushin, L. I.; Skvortsov, A. M. J Chem Phys 2008, 128, 234902 1–234902 11.

15 Daoulas, K. C.; Mueller, M.; Stoykovich, M. P.; Papakonstantopoulos, Y. J.; De Pablo, J. J.; Nealey, P. F.; Park, S. M.; Solak, H. H. J Polym Sci Part B: Polym Phys 2006, 44, 2589–2604.

16 Nunnery, G.; Hershkovits, E.; Tannenbaum, A.; Tannenbaum, R. Langmuir 2009, 25, 9157–9163.

17 Masuda, H.; Fukuda, K. Science 1995, 268, 1466–1468.

18 Furneaux, R. C.; Rigby, W. R.; Davidson, A. P. Nature 1989, 337, 147–149.

19 Doll, T.; Hochberg, M.; Barsic, D.; Scherer, A. Sens Actuators 2000, 87, 52–59.

20 Zacharatos, F.; Gianneta, V.; Nassiopoulou, A. G. Nanotechnology 2008, 19, 495306 1–495306 5.

21 Zhang, X.; Hao, Y.; Meng, G.; Zhang, L. J Electrochem Soc 2005, 152, C664–C668.

22 Choi, J.; Luo, Y.; Wehrspohn, R. B.; Hillebrand, R.; Schilling, J.; Gosele, U. J Appl Phys 2003, 94, 4757–4762.

23 Hernandez-Velez, M.; Pirota, K. R.; Paszti, F.; Navas, D.; Climent, A.; Vazquez, M. Appl Phys A 2005, 80, 1701–1706.

24 Duan, H.; Gnanaraj, J.; Chen, X.; Li, B.; Liang, J. J Power Sources 2008, 185, 512–518.

25 Koutsioubas, A. G.; Spiliopoulos, N.; Anastassopoulos, D.; Vradis, A. A.; Priftis, G. D. J Appl Phys 2008, 103, 094521-1–094521-6.

26 Koutsioubas, A. G.; Spiliopoulos, N.; Anastassopoulos, D. L.; Vradis, A. A.; Toprakcioglu, C.; Priftis, G. J Polym Sci Part B: Polym Phys 2006, 44, 1580–1591.

27 Taunton, H. J.; Toprakcioglu, C.; Fetters L. J.; Klein, J. Macromolecules 1990, 23, 571–580.

28 Motschmann, H.; Stamm, M.; Toprakcioglu, C. Macromolecules 1991, 24, 3681–3688.

29 Field, J. B.; Toprakcioglu, C.; Ball, R. C.; Stanley, H. B.; Dai, L.; Barford, W.; Penfold, J.; Smith, G.; Hamilton, W. Macromolecules 1992, 25, 434–439.

30 Siokou, A.; Papaefthimiou, V.; Kennou S. Surf Sci 2001, 482–485, 1186–1191.

31 Crank, J. The Mathematics of Diffusion, 2nd ed.; Oxford University Press: Oxford, 1979; Chapter 2, pp 20–35.

32 Carmesin, I.; Kremer, K. Macromolecules 1988, 21, 2819–2823.

33 Deutsch, H. P.; Binder, K. J Chem Phys 1991, 94, 2294–2304.

34 Koutsioubas, A. G.; Spiliopoulos, N.; Anastassopoulos, D. L.; Vradis, A. A.; Toprakcioglu, C. J Chem Phys 2009, 131, 044901-1–044901-7.

35 Kent, M. S.; Lee, L. T.; Farnoux, B.; Rondelez, F. Macromolecules 1992, 25, 6240–6247.

36 Higo, Y.; Ueno, N.; Noda, I. Polym J 1983, 15, 367–375.